Evaluation of Cooperative Interactions between Substructures of Iso-1-Cytochrome *c* Using Double Mutant Cycles†

Eydiejo Wandschneider, Barbara N. Hammack, and Bruce E. Bowler*

Department of Chemistry and Biochemistry, 2190 East Iliff Avenue, University of Denver, Denver, Colorado 80208-2436

Received June 4, 2003; Revised Manuscript Received July 11, 2003

ABSTRACT: A double mutant cycle has been used to evaluate interaction energies between the global stabilizer mutation asparagine 52 → isoleucine (N52I) in iso-1-cytochrome *c* and mutations producing single surface histidines at positions 26, 33, 39, 54, 73, 89, and 100. These histidine mutation sites are distributed through the four cooperative folding units of cytochrome *c*. The double mutant cycle starts with the iso-1-cytochrome *c* variant AcTM, a variant with no surface histidines and with asparagine at position 52. Isoleucine is added singly at position 52, AcTMI52 variant, as are the surface histidines, AcHX variants, where X indicates the histidine sequence position. The double mutant variants, AcHXI52, provide the remaining corner of the double mutant cycle. The stabilities of all variants were determined by guanidine hydrochloride denaturation and interaction energies were calculated between position 52 and each histidine site. Six of the seven double mutants show additive (AcH33I52, AcH39I52, AcH54I52, AcH89I52, and AcH100I52) stability effects or weak interaction energies (AcH73I52) of the histidine mutations and the N52I mutation, consistent with cooperative effects on protein folding and stability being sparsely distributed through the protein structure. The AcH26I52 variant shows a strong favorable interaction energy, 2.0 ± 0.5 kcal/mol, between the N52I mutation in one substructure and the addition of His 26 to an adjacent substructure. The data are consistent with an entropic stabilization of the intersubstructure hydrogen bond between His 26 and Glu 44 by the Ile 52 mutation.

Protein folding can be viewed at as a cooperative process in which a single mutation can drastically affect the stability and functionality of a protein. Networks of residues have been shown to be evolutionarily conserved in proteins where distant communication is necessary for protein function (*1*), indicating that small, yet specific, changes in the sequence of amino acid residues can drastically change the structure and function of proteins. Studies on the native-state hydrogen exchange monitored folding of ribonuclease HI and cytochrome *c* have shown that mutations not only affect the site of the mutation but also portions of the protein distal to the site of mutation, demonstrating that conformational energy can propagate across long distances in proteins (*2*, *3*). Cytochrome *c*, like many proteins, is known to have a two-state thermodynamic transition (*4*), which indicates that the folding pathway has a single transition state and is either fully folded or unfolded.

A high-resolution three-dimensional X-ray structure (*5*) for the mutation of asparagine at position 52 to isoleucine (N52I)[1] in iso-1-cytochrome *c* is consistent with the ability of this mutation to dramatically increase the stability of the protein (*6*). The mutation of Asn to Ile displaces an internally bound water molecule (W166), simultaneously altering a hydrogen bond network. In its place, Tyr 67 shifts toward Thr 78, which causes their hydroxyl groups to hydrogen bond. This new network of hydrogen bonds, along with the loss of a buried water, greatly increases the stability in both oxidation states (*5*, *6*).

In the process of adding N52I to relatively unstable single histidine variants of iso-1-cytochrome *c*, this lab was able to increase the stability of these variants and in turn discovered differential cooperative activity between position 52 and two histidine mutation sites. When the N52I mutation was added to the variant AcH54 (N-terminally acetylated variant of iso-1-cytochrome *c* with a single surface histidine at position 54, see ref *7*), the free energy of unfolding increased by ∼2 kcal/mol (*8*); adding the same mutation to the AcH26 variant (*7*) increased the stability by ∼4 kcal/mol (*8*). What is the reason for the large difference in stabilization? Is the effect due to a favorable cooperative

† This work was supported in part by NIH Grant GM57635 (B.E.B.). Acknowledgment is made to the donors of the Petroleum Research Fund (38865-AC4, B.E.B.) administered by the American Chemical Society for partial support of the work. The Beckman CEQ8000 was purchased with NSF Grant DBI 9977691. The Applied Photophysics PiStar 180 Spectrometer was purchased with NIH Grant 1 S10 RR16632-01.

* To whom correspondence should be addressed. Phone: (303) 871−2985. Fax: (303) 871−2254. E-mail: bbowler@du.edu.

[1] Abbreviations: N52I, asparagine at position 52 changed to isoleucine; AcTM, variant of iso-1-cytochrome *c* with no surface histidines and with N-terminal acetylation, relative to the wild-type sequence this protein carries the mutations, T(−5)S, K(−2)L, H26N, H33N, H39Q, C102S; AcTMI52, AcTM variant of iso-1-cytochrome *c* with an isoleucine replacing asparagine at position 52. AcHX, variant of iso-1-cytochrome *c* derived from the AcTM variant by adding a surface histidine at position X; AcHXI52, AcHX variant of iso-1-cytochrome *c* with an isoleucine replacing asparagine at position 52; gdnHCl, guanidine hydrochloride; $C_{1/2}$, midpoint of guanidine hydrochloride unfolding titration; $\Delta\Delta G_{double}$, stability difference caused by double mutation; $\Sigma\Delta\Delta G_{single}$, summed stability effects of single mutants; *m*, slope of the dependence of free energy of unfolding on guanidine hydrochloride concentration.

10.1021/bi034958t CCC: $25.00
Published on Web 08/16/2003

interaction between positions 26 and 52, or a negative cooperative interaction between positions 52 and 54?

Thermodynamic cycles have been used to discern how functions in proteins are linked (*9*). They have been utilized to investigate ligand binding and protein folding as well as mutational effects on structure−function relationships in proteins. To look at the effect of one mutation in a protein and how the mutation affects other sites, either near the site of mutation or further along in the amino acid sequence, double mutant cycles have been utilized. This method allows for investigation of how mutations interact to change the global stability of the protein (*10*−*12*). The double mutant cycle technique is employed here to look at the effect of Ile 52 on a large set of single histidine variants distributed throughout the structure of cytochrome *c*. Using this set of double mutant cycles, we have observed that strong energetic connectivity of position 52 to other sites in the protein is sparsely distributed, as is observed using evolutionary methods (*1*).

MATERIALS AND METHODS

Site-Directed Mutagenesis. For preparation of AcHXI52 variants, single-stranded pRS/C7.8 DNA containing the AcTMI52 variant of iso-1-cytochrome *c* was used as a template for oligonucleotide directed mutagenesis using the method of unique restriction site elimination (*13*) as previously described (*7*, *14*). Mutated DNA sequences were confirmed using a Beckman CEQ8000 automated DNA sequencer and the mutated double-stranded DNA was then transformed into the cytochrome *c* deficient GM-3C-2 strain of *Saccharamyces cerevisiae* and the functionality of the iso-1-cytochrome *c* variant confirmed by phenotypic screening (*15*). A curing procedure was then used to confirm that the cytochrome *c* was being expressed from the pRS/C7.8 phagemid (*15*, *16*). The pRS/C7.8 vector was then rescued from the *S. cerevisiae* cells and resequenced to determine if unwanted mutations occurred, under the conditions of selective pressure used to express iso-1-cytochrome *c* in yeast (*16)*. All variants contain the mutation C102S to prevent intermolecular disulfide bond formation during physical studies.

Protein Isolation and Purification. Yeast media was inoculated in a New Brunswick BioFlo IIC fermentor with yeast carrying the mutated cytochrome *c* gene in the pRS/C7.8 vector; the yeast cells were grown to saturation. The cells were then harvested and lysed using a 2:1 mixture of 1 M NaCl and ethyl acetate (*15*, *16*). The lysate was separated from cell debris and treated with 50% ammonium sulfate followed by dialysis using 3500 MW cutoff dialysis tubing in 12.5 mM sodium phosphate buffer, pH 7.2, 1 mM EDTA, 2 mM β-mercaptoethanol. CM sepharose cation exchange chromatography and high-resolution cation exchange HPLC further completed purification of the proteins (*16*, *17*).

Stability Measurements. Protein unfolding was monitored by circular dichroism spectroscopy (Applied Photophysics PiStar 180 spectrometer), using the ellipticity value at 222 nm and a baseline reference at 250 nm. Titrations were carried out with 20 mM Tris, pH 7.0, and 40 mM NaCl as buffer. The protein concentration was approximately 4 μM. The concentration of gdnHCl in protein samples was adjusted by using a Hamilton Microlab 500 series titration system, which automatically withdraws a small volume of the sample and replaces it with 6 M gdnHCl containing the same Tris/NaCl buffer and 4 μM protein. The concentration of gdnHCl ranged from 0.0 to 3.5 M in increments of 0.1 M, except in the transition region where the increments were 0.05 M. The sample cell was maintained at 25 ± 0.1 °C using a circulating water bath (ThermoNESLAB RTE7) and jacketed cell holder. The ellipticity as a function of concentration of gdnHCl, [gdnHCl], was fit to a two-state unfolding model with SigmaPlot, v. 7, software using nonlinear least-squares methods (Figure 1, eq 1, see ref *7*).

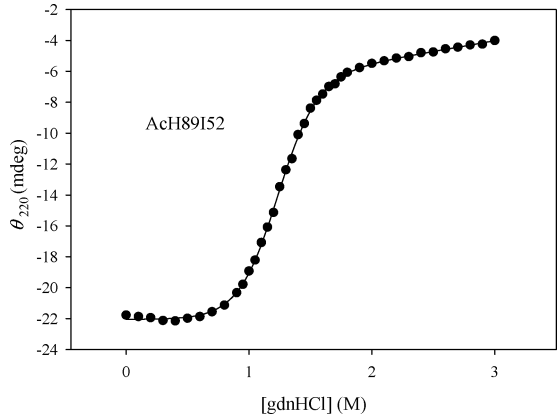

FIGURE 1: Denaturation curve for AcH89I52 iso-1-cytochrome *c* at pH 7.0 (20 mM Tris, 40 mM NaCl) and 25 °C. Ellipticity at 222 nm is plotted against [gdnHCl]. The continuous curve is the nonlinear least-squares fit to eq 1.

$$\theta = \frac{\theta_N^\circ + \{(\theta_D^\circ + m_D[\text{gdnHCl}])e^{(m[\text{gdnHCl}]-\Delta G_u(H_2O))/RT}\}}{1 + e^{(m[\text{gdnHCl}]-\Delta G_u(H_2O))/RT}} \quad (1)$$

Equation 1 fits native state (θ_N°) and denatured state ($\theta_D^\circ + m_D$[gdnHCl]) baselines as well as the unfolding transition region simultaneously, assuming a linear dependence of free energy on [gdnHCl] (eq 2, see ref *18*).

$$\Delta G_u = \Delta G_u(H_2O) - m[\text{gdnHCl}] \quad (2)$$

The values for stability in water, $\Delta G_u(H_2O)$, and denaturant dependence of the free energy of unfolding (*m*-value) were determined from the fits of the data to eq 1. The errors reported are the standard deviation for three separate experiments.

Calculation of Interaction Energies. The energy of interaction is defined as the difference between the stability change caused by double mutation, $\Delta\Delta G_{double}$, and the summed stability effects of the single mutations, $\Sigma\Delta\Delta G_{single}$ (Figure 2). To examine the interactions of multiple side chain residues, Fersht and Horovitz (*10*) laid out a general theory. Equation 3 defines the interaction energy, $\Delta^2 G_{int}$, for the interaction of two side chains in the double mutant cycle used here (*10*).

$$\Delta^2 G_{int} = \Delta\Delta G_{double} - (\Delta\Delta G_{single1} + \Delta\Delta G_{single2}) \quad (3)$$

Calculation of Interaction Energy Error. The experimental error of $\Delta G_u(H_2O)$ is the standard deviation of three separate experiments. When calculating the interaction energies, $\Delta^2 G_{int}$, there is an accumulation of errors. The error in $\Delta^2 G_{int}$

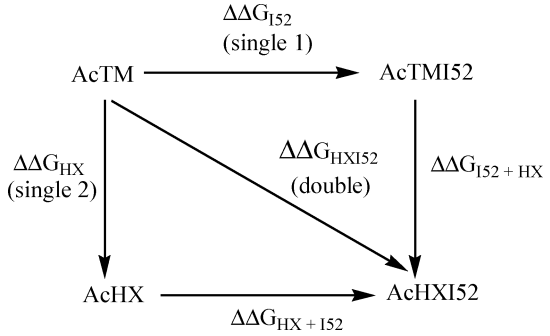

FIGURE 2: Thermodynamic cycle used to evaluate the possible interactions between the single histidine mutations (HX) and Ile 52 (I52). Free energies were determined from circular dichroism data and the $\Delta\Delta G$ values ($\Delta G_u(H_2O)_{final} - \Delta G_u(H_2O)_{initial}$) are the change in free energy of unfolding between the variants.

is equal to the square root of the sum of the square of the error in each component. Each stability change is defined as $\Delta\Delta G = \Delta G_u(H_2O)_{mutant} - \Delta G_u(H_2O)_{AcTM}$; therefore, each component of the equation for $\Delta^2 G_{int}$ above has the common constituent $\Delta G_u(H_2O)_{AcTM}$. Substituting the expression for $\Delta\Delta G$ into the equation for $\Delta^2 G_{int}$ we have

$$\Delta^2 G_{int} = \Delta G_u(H_2O)_{double} - \Delta G_u(H_2O)_{AcTM} - \{(\Delta G_u(H_2O)_{single1} - \Delta G_u(H_2O)_{AcTM}) + (\Delta G_u(H_2O)_{single2} - \Delta G_u(H_2O)_{AcTM})\} \quad (4)$$

After $\Delta G_u(H_2O)_{AcTM}$ terms are canceled, the equation can be rearranged to

$$\Delta^2 G_{int} = \Delta G_u(H_2O)_{double} - \Delta G_u(H_2O)_{single1} - \Delta G_u(H_2O)_{single2} + \Delta G_u(H_2O)_{AcTM} \quad (5)$$

Therefore, the error in $\Delta^2 G_{int}$ for AcHXI52 variants is determined by eq 6 (*11*):

$$\sigma_{\Delta^2 G_{int}} = \sqrt{(\sigma_{\Delta G_u(H_2O)_{double}})^2 + (\sigma_{\Delta G_u(H_2O)_{single1}})^2 + (\sigma_{\Delta G_u(H_2O)_{single\ 2}})^2 + (\sigma_{\Delta G_u(H_2O)_{AcTM}})^2} \quad (6)$$

In general, $\Delta^2 G_{int}$ is ~0.4 kcal/mol for the experiments reported here. Therefore, when $\Delta^2 G_{int}$ falls in the range of ±0.4 kcal/mol the effects of adding I52 and a single surface histidine to the AcTM variant are additive.

RESULTS

Creating a thermodynamic cycle of double mutants of cytochrome *c* allows us to look at possible interactions between single histidine mutations (positions 26, 33, 39, 54, 73, 89, and 100) and a stabilizing mutation at position 52 (Ile 52). Figure 2 shows the thermodynamic cycle that was constructed. The cycle starts with AcTM, a variant of iso-1-cytochrome *c* with no surface histidines. The upper horizontal branch adds an isoleucine at position 52, the left vertical branch adds a single histidine at position X, and the remaining vertical and horizontal branches add the second mutations to complete the thermodynamic cycle. The free energy of unfolding was determined for each protein in the cycle using CD spectroscopy and the corresponding free energy of interaction was determined using eq 3.

Table 1: Thermodynamic Parameters from GdnHCl Denaturation of Iso-1-cytochrome *c* Variants[a]

variant	$\Delta G_u(H_2O)$[b] (kcal/mol)	*m*-value[c] (kcal/mol M)	$C_{1/2}$[d] (M)
AcTM[e]	3.93 ± 0.15	3.71 ± 0.18	1.06 ± 0.04
AcTMI52	6.63 ± 0.23	3.82 ± 0.19	1.74 ± 0.06
AcH26[e]	4.71 ± 0.16	4.63 ± 0.15	1.02 ± 0.03
AcH33[e]	3.85 ± 0.06	4.27 ± 0.11	0.90 ± 0.01
AcH39[e]	3.16 ± 0.15	4.27 ± 0.15	0.74 ± 0.04
AcH54[e]	1.70 ± 0.08	3.93 ± 0.20	0.43 ± 0.02
AcH73[e]	2.25 ± 0.04	2.79 ± 0.09	0.81 ± 0.01
AcH89[e]	2.04 ± 0.06	3.67 ± 0.07	0.56 ± 0.03
AcH100[e]	2.81 ± 0.07	3.46 ± 0.08	0.81 ± 0.02
AcH26I52	9.37 ± 0.24	4.99 ± 0.15	1.88 ± 0.05
AcH33I52	6.47 ± 0.17	4.17 ± 0.21	1.55 ± 0.04
AcH39I52	6.29 ± 0.25	4.39 ± 0.26	1.43 ± 0.06
AcH54I52	3.93 ± 0.02	3.96 ± 0.02	0.99 ± 0.01
AcH73I52	4.40 ± 0.08	3.71 ± 0.01	1.18 ± 0.02
AcH89I52	4.43 ± 0.10	3.53 ± 0.21	1.25 ± 0.02
AcH100I52	5.51 ± 0.15	3.66 ± 0.17	1.51 ± 0.04

[a] All data collected at 25 °C in 20 mM Tris, pH 7.0, 40 mM NaCl. [b] Free energy difference between the native and denatured states in units of kilocalories per mole. [c] The *m*-value is the change in free energy with respect to the change in [gdnHCl]. [d] Midpoint concentration, $C_{1/2}$, is the [gdnHCl] at which half of the protein is denatured in units of molar. [e] Data from ref *7*.

In previous work (*7*), seven single histidine variants of cytochrome *c* were constructed placing histidines at positions 26, 33, 39, 54, 73, 89, and 100, and their stabilities measured. In this work, a second mutation was made to these single histidine variants, at position 52 and the stability was measured (Table 1); these values correspond to the bottom two corners of the thermodynamic cycle. Stability data for AcTM (*7*) and AcTMI52 provide the top corners of the thermodynamic cycle. In previous studies, it was shown that the N-terminal amino group of cytochrome *c* competes with histidine for binding to the sixth coordination site of the heme under denaturing conditions (*19*); therefore, the variants studied all have an acetylated N-terminal amino group which alleviates this problem. At pH 7.0, in the denatured state, the sixth coordination site of the heme is occupied by water (AcTM, AcTMI52) or by the single surface histidine (AcHX, AcHXI52), as indicated by studies of loop formation in the denatured state (*7*, *8*). The fifth coordination site of the heme is occupied by His 18 in both the native and the denatured state.

Guanidine Hydrochloride Denaturation Data. A summary of the gdnHCl denaturation data for all single histidine mutants, double mutants (see also Figure 1), AcTM, and AcTMI52 is given in Table 1. Stabilities ($\Delta G_u(H_2O)$) of the single histidine variants varied from 1.70 to 4.71 kcal/mol. Only one of the variants (AcH26) has a stability higher than AcTM. The *m*-values of the single histidine variants range from 2.79 to 4.63 kcal/mol M. The midpoint concentration, $C_{1/2}$, range is 0.43−1.02 M. Adding the asparagine to isoleucine mutation at position 52 increased the stability range to 3.93−9.37 kcal/mol. All of the AcHXI52 variants show an increase in stability compared to their AcHX counterparts, but only AcH26I52 showed an increase when compared to AcTMI52. The *m*-value range for the double mutants is 3.53−4.99 kcal/mol M. The midpoint concentration range, $C_{1/2}$, for double mutants is 0.99−1.88 M. In both the single mutants and the double mutants, the $\Delta G_u(H_2O)$

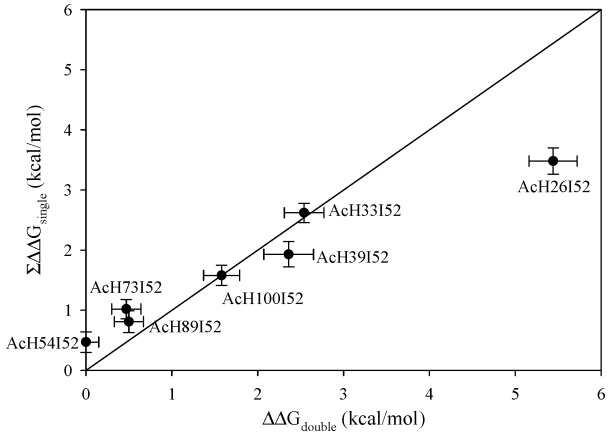

FIGURE 3: Plot of $\Sigma\Delta\Delta G_{single}$ (kcal/mol) versus $\Delta\Delta G_{double}$ (kcal/mol). The solid line is the theoretical line with a slope of one for additive effects of the two mutations.

Table 2: Interaction Free Energy Data for Single Histidine, Isoleucine 52, Double Mutants

double mutant	$\Delta\Delta G_{double}$[a]	$\Sigma\Delta\Delta G_{single}$[b]	$\Delta^2 G_{int}$[c]
AcH26I52	5.44	3.48	2.0 ± 0.5
AcH33I52	2.54	2.62	-0.1 ± 0.4
AcH39I52	2.36	1.93	0.4 ± 0.5
AcH54I52	0.00	0.47	-0.5 ± 0.4
AcH73I52	0.47	1.02	-0.6 ± 0.4
AcH89I52	0.50	0.81	-0.3 ± 0.4
AcH100I52	1.58	1.58	0.0 ± 0.4

[a] Difference in free energy between the free energy of the protein with double substitutions and the free energy of the AcTM variant, $\Delta\Delta G = \Delta G_u(H_2O)_{double} - \Delta G_u(H_2O)_{AcTM}$. [b] The sum of the $\Delta\Delta G_{single}$ values of corresponding single substitutions, where $\Delta\Delta G_{single} = \Delta G_u(H_2O)_{single} - \Delta G_u(H_2O)_{AcTM}$. [c] $\Delta^2 G_{int} = \Delta\Delta G_{double} - \Sigma\Delta\Delta G_{single}$.

and $C_{1/2}$ values decrease as the histidine is moved further from the site of heme attachment to the polypeptide chain (Cys 14, Cys17), reaching a low point for His 54, then increasing again. Also notable is a steady decrease in *m*-values as the denatured state histidine heme loop size increases.

Additivity of Stability. The stability changes for double mutants relative to AcTM ($\Delta\Delta G_{double}$) are compared to the sum of the stability changes of corresponding single mutants ($\Sigma\Delta\Delta G_{single}$), by plotting $\Sigma\Delta\Delta G_{single}$ against the stability changes of double mutants, $\Delta\Delta G_{double}$ (Figure 3). The solid line in Figure 3 is the theoretical line with a slope of one on which all points would line up if additivity were ideal. Data points above the line correspond to negative interaction energies and those below correspond to positive interactions energies. A linear regression of the $\Sigma\Delta\Delta G_{single}$ versus the $\Delta\Delta G_{double}$ data points gives a slope of 0.68 and an r^2 of 0.94. Most of the data points line up with the theoretical line, indicating a uniform trend of additive stability with the addition of Ile 52. AcH26I52 deviates strongly from the ideal line, indicating a strong positive interaction between the mutation at position 26 and the mutation at position 52.

The calculated energies of interaction, $\Delta^2 G_{int}$, are shown in Table 2. If $\Delta^2 G_{int}$ is equal to or less than ± 0.4 kcal/mol, the calculated error, then the double mutant is considered to have additive stability effects and no significant interaction energy exists between the two mutations. If $\Delta^2 G_{int}$ is a positive value, the interactions between the positions of mutation reinforce each other. Conversely, if $\Delta^2 G_{int}$ is a negative value, the positions of mutation have a negative effect on each other. AcH26I52 has a large positive $\Delta^2 G_{int}$, indicating reinforcing interactions between the mutations at positions 26 and 52. It should be noted that it cannot be determined directly from double mutant cycle analysis whether the positive $\Delta^2 G_{int}$ between positions 26 and 52 is due to a stabilizing interaction in the native state or a destabilizing interaction in the denatured state. The other HisX/I52 pairs give $\Delta^2 G_{int}$ within error of zero. Therefore, the N52I mutation stabilizes these single histidine variants, however, there is no added interaction positive or negative. It is possible that a small negative interaction could be taking place between positions 73 and 52, due to a slightly negative $\Delta^2 G_{int}$ (see Table 2).

DISCUSSION

Denatured State Effects on the Thermodynamic Cycle. Hammack et al. (*7*) used pK_a(obs) values to look at the strength of the histidine−heme bond under denaturing conditions. They observed a trend in which the most stable loop to be formed (lowest pK_a(obs)) occurs with the AcH54 variant. Increasing loop sizes (His at positions 73, 89, and 100) decreased loop stability linearly as a function of the logarithm of loop size, whereas decreasing loop sizes (His at positions 39, 33, and 26) also decreased loop stability. This trend indicates a strong denatured state stabilization with a histidine in position 54 and less stabilization going out in either direction from this sequence position. This phenomenon is unaffected by the I52 mutation; the denatured state pK_a(obs) values for loop formation are identical, within error, for corresponding AcHX and AcHXI52 variants in 3 M gdnHCl (*8*, Wandschneider and Bowler, unpublished results), indicating no significant effect of the N52I mutation on denatured state energetics. Stability experiments are performed at pH 7.0 to ensure that the primary ligand to the heme under denaturing conditions is histidine. Interestingly, the denatured state data mirror the observed trends in global stability for both the single histidine variants and their I52 counterparts. There is a definite minimum in global stability with position 54 variants (most stable denatured state) in both the AcHX variants and once I52 is added (see Table 1). Likewise, both larger and smaller "loop size" variants show an increasing global stability moving away in both directions from position 54. The same trend observed for $\Delta G_u(H_2O)$ is also seen in $C_{1/2}$ (Table 1). The correlation of denatured state loop stability with the $\Delta G_u(H_2O)$ and the $C_{1/2}$ values indicates that the denatured state strongly impacts global stability for these variants.

There is also significant evidence that *m*-values are related to the extent of compactness or residual structure in the denatured state (*20*, *21*). A histidine ligated to the heme in the denatured state of iso-1-cytochrome *c* forms a loop that constrains the polypeptide. As a result of this constraint, a more compact denatured state is believed to be formed. The decrease in *m*-values as loop size increases was seen previously for single histidine variants (*7*), and is observed here for the double mutation variants. This observed trend in *m*-values is also consistent with an impact of the denatured state on overall stability.

Do these denatured state effects on stability have an impact on $\Delta^2 G_{int}$? To determine this, we must carefully consider

both the thermodynamic cycle (Figure 2) and the equation for interaction energy (eq 3). When a histidine is present in a variant a loop is formed in the denatured state and the denatured state stability is affected. If there is no histidine, no loop can form (at pH 7.0) and no loop related effects on denatured state stability can occur. The term $\Delta\Delta G_{double}$ is defined as the difference between the free energies of AcHXI52 (loop formed) and AcTM (no loop formed) and therefore contains one denatured state loop formation factor. The term $\Sigma\Delta\Delta G_{single}$ is the sum of $\Delta\Delta G_{single\ 1}$ ($\Delta G_{AcTMI52} - \Delta G_{AcTM}$, no loops) and $\Delta\Delta G_{single\ 2}$ ($\Delta G_{AcHX} - \Delta G_{AcTM}$, loop formed for AcHX). Since $\Sigma\Delta\Delta G_{single}$ contains one denatured state loop effect and it is subtracted from $\Delta\Delta G_{double}$, which also contains a single denatured state loop effect factor, then the two denatured state loop factors should cancel each other out and therefore have no effect on the interaction energy calculation. As indicated above, the N52I mutation does not significantly affect that stability of the denatured state, since experiments on the thermodynamics of denatured state loop formation show similar pK_a(obs) values for corresponding AcHX and AcHXI52 variants (*7*, *8*, Wandschneider and Bowler unpublished results*)*. Since corresponding AcHX and AcHXI52 variants are always being compared in each double mutant cycle (for example, AcH26 and AcH26I52), the cancellation of the denatured state loop effect described above should be nearly exact. In 3 M gdnHCl, the denatured state pK_a(obs) for lysine−heme loop formation is 7.62 ± 0.05 for AcTM (*14*) and 7.63 ± 0.03 for AcTMI52 (Wandschneider and Bowler, unpublished results) indicating no detectable effect on the open loop form of the denatured state of iso-1-cytochrome *c* due to addition of the N52I mutation. Thus, our denatured state histidine−heme and lysine−heme loop formation assays (*7*, *14*) provide no evidence for an effect of the N52I mutation on the energetics of the gdnHCl denatured state of iso-1-cytochrome *c*.

General Observations on Δ^2G_{int}. Horse heart cytochrome *c* is known to have four folding units called substructures. They have been color coded in order of increasing free energy level red to blue as follows: red, 70−85 loop; yellow, 36−61 loop; green, 20−35 loop and 60's helix; and blue, amino terminal helix and carboxyl-terminal helix (Figure 4, ref *22*). Hydrogen exchange experiments as a function of [gdnHCl], used to define these substructures, have not been performed on yeast iso-1-cytochrome *c*, although NMR-monitored hydrogen−deuterium exchange data in aqueous buffer show a qualitative link between the substructures of horse heart cytochrome *c* and yeast iso-1-cytochrome *c* (*23*). For oxidized iso-1-cytochrome *c*, the most protected section of the protein is the N and C terminal helices, and next protected is loop A and the 60's helix which is consistent with the blue and green substructures found in the horse protein. However, a discrepancy is seen when comparing the red and yellow substructures in yeast versus horse. Much of the yellow substructure is poorly protected against hydrogen exchange in yeast suggesting that it may be less stable than the red substructure in yeast iso-1-cytochrome *c* (*23*). Recent work done in this lab on the alkaline conformational transition of a His 73 iso-1-cytochrome *c* variant also indicates that the red substructure acts as a cooperative folding unit in yeast iso-1-cytochrome *c* (*24*−*26*). The thermodynamic parameters (*m*-value, ΔC_p, see refs *24* and *25*) for the His 73 driven partial unfolding of His 73 iso-1-cytochrome *c* are quantitatively consistent with those for the red substructure of horse heart cytochrome *c* (*22*). Therefore, there is substantial evidence that the substructures defined for horse heart cytochrome *c* can, for the most part, be applied to the yeast protein.

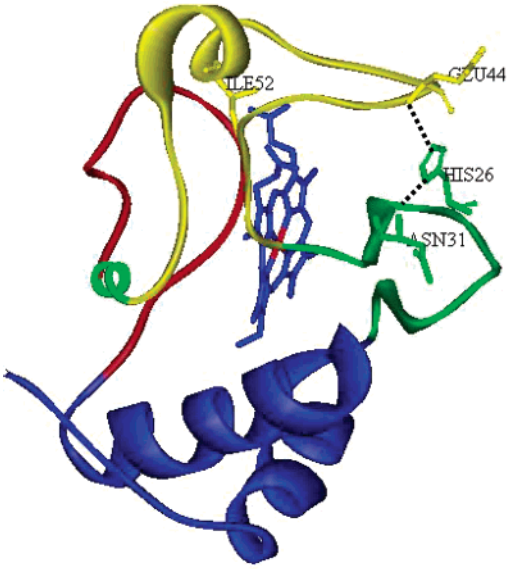

FIGURE 4: Substructures of horse cytochrome *c*, color coded in order of increasing free energy level (red, yellow, green, and blue, see ref *22*), superimposed on the structure of yeast iso-1-cytochrome *c*. Amino acids His 26, Asn 31, Glu 44, and Ile 52 are depicted with stick representations. The hydrogen bonds between the His 26 imidazole ring and the backbone carbonyl of Glu 44 and the amide NH of Asn 31 are shown with dashed lines. In the oxidized N52I, C102T iso-1-cytochrome *c* structure (*5*), pdb1crg.ent, the distance of closest approach between the side chains of histidine 26 and isoleucine 52 is 11.78 Å.

In our double mutant cycle study, we have included surface histidines from each of the substructures defined for the horse protein, allowing cooperative interactions between position 52 and all substructures to be probed. Three of these histidines are part of the wild-type sequence (positions 26, 33, and 39). Position 52 is located in the yellow substructure. We find that five out of seven of the double mutation variants give additive effects for the two mutations, within error, consistent with the observation that pathways of strong allosteric energetic conductivity are sparse (*1*). Only His 26 has a strong positive interaction energy with the Ile 52 mutation, whereas His 73 shows a weak negative interaction with the Ile 52 mutation.

Negative Interaction between Positions 52 and 73. AcH73 deviates from the trends seen in free energies, midpoint concentration, and *m*-value, but with the addition of I52, the double mutant conforms to the trends in these parameters. It has been shown previously that a His 73 variant has a three-state alkaline conformational transition, which is consistent with CD-monitored unfolding occurring from a partially unfolded state (*24*−*27*). The AcH73 variant likely behaves similarly, which is apparent from the low *m*-value observed for this variant (Table 1). With isoleucine at position 52, the His 73 variant appears to unfold from a fully native state (*26*). Since the AcH73 and AcH73I52 variants are not unfolding from the same native state, the small negative value for Δ^2G_{int} should be interpreted with caution.

Positive Interaction between Positions 26 and 52. As discussed above, none of our denatured state data (*7*, *8*, *14*)

provide evidence that interactions in the denatured state cause the strong positive Δ^2G_{int} between positions 26 and 52. Therefore, we focus our attention on the native state structure to provide an explanation for the observed Δ^2G_{int}. A histidine at position 26 is highly evolutionarily conserved (in 87 out of 96 mitochondrial cytochromes *c*, see ref *28*) making it important for the structure and function of the protein. His 26 is not directly involved in regular secondary structure such as α-helix and *β*-sheet; however, the imidazole group of histidine 26 forms a hydrogen bond with the backbone carbonyl group of Glu 44 as well as a backbone amide nitrogen atom of Asn 31 (Figure 4, see ref *29*). Mutational studies in which His 26 was replaced by other amino acids suggest a decrease in stability and in the ability of the protein to function; these effects have been attributed to an increase in the mobility of surface loops (*30*−*32)*. In analysis of ligand mediated cooperative interactions between domains, Freire and co-workers (*33*) showed that stabilization of a less stable domain strongly enhanced the stability of a more stable domain through cooperative interactions. Communication of stability downward from the more stable to the less stable domain was less effective (*33*). Position 26 is found in the green substructure of cytochrome *c*, which is the second most stable substructure, whereas position 52 resides in the second least stable substructure (*22*). A similar mechanism for allosterism could be operative between the histidine at position 26, which resides in a more stable substructure and the isoleucine at position 52. The addition of Ile 52 to the less stable substructure could reinforce the His 26 in the more stable substructure, and add to the overall global stability of the double mutant protein. Although, this analysis indicates that a cooperative interaction between Ile 52 and His 26 could easily occur, similar effects are not observed for other histidines in more stable substructures, His 89 and His 100. Therefore, the reason for a cooperative effect on stability must be more specific.

Without an isoleucine at position 52, X-ray diffraction, NMR monitored hydrogen/deuterium exchange, and ^{15}N relaxation data have shown that the yellow substructure is the most dynamic part of oxidized iso-1-cytochrome *c* (*23*, *29*, *34*, *35*). The dynamics of the yellow substructure would be expected to weaken the hydrogen bonding between His 26 and Glu 44 in this substructure and therefore lower stability. The X-ray structure of N52I, C102T iso-1-cytochrome *c* indicates that the I52 mutation specifically stabilizes the yellow substructure, forming a new hydrogen bonding network and reducing substructural fluctuation (*5*). This increased rigidity should decrease the entropic cost of forming the Glu 44/His 26 hydrogen bond. Therefore, a strong interaction energy between the N52I and N26H mutations is expected. Similar entropic effects have been used to explain interaction energies in three residue salt bridges (*10*).

For thermal denaturation of iso-2-cytochrome *c* (*36*), a thermodynamic cycle involving direct electrochemical reduction of the N52I variant in both the native and the denatured state indicates that a significant destabilization of the denatured state of the N52I variant relative to the wild-type protein contributes to the stabilizing effect of this mutation. The authors note that similar effects on the electrochemical reduction of the denatured state are not observed for the N52I mutation under gdnHCl denaturation conditions (*36*, *37*), implying that the N52I mutation has no significant effect on the denatured state in the presence of gdnHCl. Our histidine−heme loop formation data in 3 M gdnHCl for AcHX versus AcHXI52 variants (see above) are also consistent with no effect of the N52I mutation on the gdnHCl denatured state. Thus, the effect of the N52I mutation on the denatured state of yeast cytochromes *c* appears to be specific to thermal denaturation conditions. While we cannot eliminate the possibility of denatured state contributions to Δ^2G_{int} that are beyond the detection of our denatured state loop formation assay (*7*, *8*, *14*), based on the available data, the native state interactions described above provide the best explanation for the strong allosteric interaction between the N52I mutation and His 26. These native state interactions are, therefore, expected to be an important contributor to the global stabilizer effect of this mutation in wild-type iso-1-cytochrome *c* (*6*).

Previously published urea denaturation data for rat cytochrome *c* (*32*) can also be used in a double mutant cycle to calculate an interaction energy, Δ^2G_{int}, for the mutational introduction of Ile 52 and His 26. Starting with a Val 26 Asn 52 variant, single mutations to His 26 or Ile 52 increase $\Delta G_u(H_2O)$ by 3.8 and 1.9 kcal/mol respectively. Simultaneous introduction of both mutations increases stability by only 0.6 kcal/mol, giving $\Delta^2G_{int} = -5.0$ kcal/mol, a large unfavorable interaction energy. The strong interaction of these mutations is consistent in both rat and yeast although the direction of the interaction is opposite. Addition of Ile 52 to the His 26 containing rat cytochrome *c* decreased the urea *m*-value to ∼60% of its value in the His 26 protein. The introduction of Ile 52 has no effect on the *m*-value in yeast iso-1-cytochrome *c* (see Table 1), except for the AcH73/AcH73I52 pair, as discussed above. The strong loss in cooperativity (decrease in *m*-value) in the rat cytochrome *c* when the Ile 52 is added to His 26 indicates that the effects of Ile 52 are very different from yeast. There are numerous amino acid substitutions in the yellow substructure of yeast iso-1 versus rat cytochrome *c* (residues 39, 40, 44, 46, 53, 54, 56−58, and 60, see ref *28*). This number of substitutions alone could impact energetic communication between positions 26 and 52. However, position 44 in the yellow substructure, which hydrogen bonds to the side chain of His 26, is a valine in rat versus a glutamate in yeast iso-1. It is possible that the increased rigidity in the yellow substructure induced by the I52 mutation (*5*) makes hydrogen bond formation less favorable due to the additional steric constraints imposed by a *β*-substituted residue at position 44 in rat cytochrome *c*. It is also possible that Ile 52 and His 26 interact so as to stabilize the denatured state of rat cytochrome *c* in urea. However, unlike the yeast protein (*8*, *36*, *37*), no data are available concerning the effect of the N52I mutation on the denatured state of the rat protein.

It has been suggested that the rigidity in the 20−35 loop of the green substructure is important for function (*30*). This suggestion is based on the decrease in cytochrome *c* function when His 26 is replaced, leading to loss of the hydrogen bonds to the main chain atoms of Asn 31 and Glu 44. The deleterious effect of loss of rigidity when His 26 is replaced is believed to be most important for the interaction with cytochrome *c* reductase (*30*). Even though addition of Ile 52 to the His 26 protein likely increases rigidity, this property appears not to have been selected for. (In fact, position 52

is strictly conserved as Asn in 96 mitochondrial cytochromes *c*, see ref *28*.) Thus, it would seem from an evolutionary standpoint that cytochrome *c* may require a balance between rigidity and flexibility to be optimized for interactions with its various redox partners.

SUMMARY

In conclusion, we used a set of double mutant cycles to investigate interactions between surface histidines and a global stabilizer mutation for iso-1-cytochrome *c*, N52I. The data show that strong stabilizing allosteric cooperative interactions are sparsely distributed throughout the protein. Only a single sequence position, out of the seven investigated, interacts other than additively with the I52 mutation. The strong favorable Δ^2G_{int} observed between I52 and H26 is consistent with entropic stabilization of an intersubstructure hydrogen bond between His 26 in the green substructure of cytochrome *c* and Glu 44 in the yellow substructure of cytochrome *c*. The results are also consistent with upward propagation of stability from dynamic, or less stable, portions of a protein to more stable portions of a protein.

Note added in Proof: After this paper was accepted for publication, Englander and co-workers (*38*) published more extensive hydrogen exchange data on horse heart cytochrome *c* which indicate that the Ile 52 mutation is within a newly defined substructure referred to as the nested yellow (N-yellow) substructure. The N-yellow substructure is less stable than the red substructure placing the Ile 52 mutation in the least stable substructure of cytochrome *c*. This revised placement of the Ile 52 mutation within the hierarchy of cooperative folding units of cytochrome *c* does not substantively affect the conclusions of this paper. However, the newly defined N-yellow substructure removes the main qualitative inconsistency between the hydrogen exchange data for yeast iso-1-cytochrome *c* and the substructure hierarchy observed for the horse protein, strengthening the case that the substructures observed for horse cytochrome *c* may be applied to yeast iso-1-cytochrome *c*.

REFERENCES

1. Suel, G. M., Lockless, S. W., Wall, M. A., and Ranganathan, R. (2003) Evolutionarily conserved networks of residues mediate allosteric communication in proteins. *Nat. Struct. Biol. 10*, 59−69.
2. Goedken, E. R., and Marqusee, S. (2001) Native-state energetics of a thermostabilized variant of ribonuclease HI. *J. Mol. Biol. 314*, 863−871.
3. Xu, Y., Mayne, L., and Englander, S. W. (1998) Evidence for an unfolding and refolding pathway in cytochrome *c*. *Nat. Struct. Biol. 5*, 774−778.
4. Privalov, P. L. (1979) Stability of protein: Small globular proteins. *Adv. Protein Chem. 33*, 167−241.
5. Berghuis, A. M., Guillemette, J. G., McLendon, G., Sherman, F., Smith, M., and Brayer, G. D. (1994) The role of a conserved internal water molecule and its associated hydrogen bond network in cytochrome *c*. *J. Mol. Biol. 236*, 786−799.
6. Das, G., Hickey, D. R., McLendon, D., McLendon, G., and Sherman, F. (1989) Dramatic thermostabilization of yeast iso-1-cytochrome *c* by an asparagine → isoleucine replacement at position 57. *Proc. Natl. Acad. Sci. U.S.A. 86*, 496−499.
7. Hammack, B. N., Smith, C. R., and Bowler, B. E. (2001) Denatured state thermodynamics: Residual structure, chain stiffness and scaling factors. *J. Mol. Biol. 311*, 1091−1104.
8. Hammack, B. N. (2000) Effects of yeast iso-1-cytochrome *c* histidine variants on denatured state energetics, Ph.D. Thesis, Department of Chemistry and Biochemistry, University of Denver, Denver, Colorado.
9. Di Cera, E. (1998) Site-specific analysis of mutational effects in proteins. *Adv. Protein Chem. 51*, 59−119.
10. Horovitz, A., and Fersht, A. R. (1992) Cooperative interactions during protein folding. *J. Mol. Biol. 224*, 733−740.
11. Chen, J., and Stites, W. E. (2001) Energetics of side chain packing in staphylococcal nuclease assessed by systematic double mutant cycles. *Biochemistry 40*, 14004−14011.
12. Spudich, G., Lorenz, S., and Marqusee, S. (2002) Propagation of a single destabilizing mutation throughout the *Escherichia coli* ribonuclease HI native state. *Protein Sci. 11*, 522−528.
13. Deng, W. P. D., and Nickoloff, J. A. (1992) Site-directed mutagenesis of virtually any plasmid by eliminating a unique site. *Anal. Biochem. 200*, 81−88.
14. Smith, C. R., Wandschneider, E., and Bowler, B. E. (2003) Effect of pH on the iso-1-cytochrome *c* denatured state: Changing constraints due to heme ligation. *Biochemistry 42*, 2174−2184.
15. Herrmann, L., Flatt, P., and Bowler, B. E. (1996) Site-directed replacement of the invariant lysine 73 of *Saccharomyces cerevisiae* iso-1-cytochrome *c* with all ribosomally encoded amino acids. *Inorg. Chim. Acta 242*, 97−103.
16. Bowler, B. E., May, K., Zaragoza, T., York, P., Dong, A., and Caughey, W. S. (1993) Destabilizing effects of replacing a surface lysine of cytochrome *c* with aromatic amino acids: Implications for the denatured state. *Biochemistry 32*, 183−190.
17. Bowler, B. E., Dong, A., and Caughey, W. S. (1994) Characterization of the guanidine hydrochloride denatured state of iso-1-cytochrome *c* by infrared spectroscopy. *Biochemistry 33*, 2402−2408.
18. Schellman, J. A. (1978) Solvent denaturation. *Biopolymers 17*, 1305−1322.
19. Hammack, B. N., Godbole, S., and Bowler, B. E. (1998) Cytochrome *c* folding traps are not due solely to histidine-heme ligation: Direct demonstration of a role for N-terminal amino group-heme ligation. *J. Mol. Biol. 275*, 715−724.
20. Dill, K. A., and Shortle, D. (1991) Denatured states of proteins. *Annu. Rev. Biochem. 60*, 795−825.
21. Shortle, D. (1995) Staphylococcal nuclease: A showcase of *m*-value effects. *Adv. Protein Chem. 46*, 217−247.
22. Bai, Y., Sosnick, T. R., Mayne, L., and Englander, S. W. (1995) Protein folding intermediates: Native state hydrogen exchange. *Science 269*, 192−197.
23. Baxter, S. M., and Fetrow, J. S. (1999) Hydrogen exchange behavior of [*U*-^{15}N]-labeled oxidized and reduced iso-1-cytochrome *c*. *Biochemistry 38*, 4493−4503.
24. Nelson, C. J., and Bowler, B. E. (2000) pH dependence of formation of a partially unfolded state of a Lys 73 → His variant of iso-1-cytochrome *c*: Implications for the alkaline conformational transition of cytochrome *c*. *Biochemistry 39*, 13584−13594.
25. Nelson, C. J., LaConte, M. J., and Bowler, B. E. (2001) Direct Detection of Heat and Cold Denaturation for Partial Unfolding of a Protein. *J. Am. Chem. Soc. 123*, 7453−7454.
26. Kristinsson, R. (2003) Inter-substructural coopertivity in iso-1-cytochrome *c*: Effects on the alkaline conformational transition. M.S. Thesis, Department of Chemistry and Biochemistry, University of Denver, Denver, Colorado.
27. Godbole, S., Dong, A., Garbin, K., and Bowler, B. E. (1997) A lysine 73 → histidine variant of yeast iso-1-cytochrome *c*: Evidence for a nativelike intermediate in the unfolding pathway and implications for *m* value effects. *Biochemistry 36*, 119−126.
28. Moore, G. R., and Pettigrew, G. W. (1990) *Cytochrome c*: *Evolutionary, Structural and Physicochemical Aspects*, pp 116−127, Springer-Verlag, New York.
29. Berghius, A. M., and Brayer, G. D. (1992) Oxidation state-dependent conformational changes in cytochrome *c*. *J. Mol. Biol. 223*, 959−976.
30. Fetrow, J. S., Dreher, U., Wiland, D. J., Schaak, D. L., and Boose, T. L. (1998) Mutagenesis of histidine 26 demonstrates the importance of loop-loop and loop-protein interactions for the function of iso-1-cytochrome *c*. *Protein Sci. 7*, 994−1005.
31. Fetrow, J. S., Horner, S. R., Oehrl, W., Schaak, D. L., Boose, T. L., and Burton, R. E. (1997) Analysis of the structure and stability of omega loop A replacements in yeast iso-1-cytochrome *c*. *Protein Sci. 6*, 197−210.
32. Qin, W., Sanishvili, R., Plotkin, B., Schejter, A., and Margolish, E. (1995) The role of histidines 26 and 33 in the structural stabilization of cytochrome *c*. *Biochim. Biophys. Acta 1252*, 87−94.

33. Luque, I., Leavitt, S. A., and Freire, E. (2002) The linkage between protein folding and functional cooperativity: Two sides of the same coin? *Annu. Rev. Biophys. Biomol. Struct. 31*, 235−256.
34. Marmorino, J. L., Auld, D. S., Betz, S. F., Doyle, D. F., Young, G. B., and Pielak, G. J. (1993) Amide protein exchange rates of oxidized and reduced *Saccharomyces cerevisiae* iso-1-cytochrome *c*. *Protein Sci. 2*, 1966−1974.
35. Fetrow, J. S., and Baxter, S. M. (1999) Assignment of ^{15}N chemical shifts and ^{15}N relaxation measurements for oxidized and reduced iso-1-cytochrome *c*. *Biochemistry 38*, 4480−4492.
36. McGee, W. A., Rosell, F. I., Liggins, J. R., Rodriguez-Ghidarpour, S., Luo, Y., Chen, J., Brayer, G. D., Mauk, A. G., and Nall, B. T. (1996) Thermodynamic cycles as probes of structure in unfolded proteins. *Biochemistry 35*, 1995−2007.
37. Komar-Panicucci, S., Weis, D., Bakker, G., Qiao, T., Sherman, F., and McLendon, G. (1994) Thermodynamics of the equilibrium unfolding of oxidized and reduced *Saccharamyces cerevisiae* iso-1-cytochrome *c*. *Biochemistry 33*, 10556−10560.
38. Krishna, M. M. G., Lin, Y., Rumbley, J. N., and Englander, S. W. (2003) Cooperative omega loops in cytochrome *c*: Role in folding and function. *J. Mol. Biol. 331*, 29−36.

BI034958T